Loss of LRP1 from GABAergic neurons impairs short-term memory function

Aaron Aykut Uner[1]*, Zhi-Shuai Hou[1]*, Ahmet Aydogan[1,7]*, Kellen Cristina da Cruz Rodrigues[1], Jennie Young[1], Anthony Choi[1], Won-Mo Yang[1], Jongkyun Kang[2], Woojin Kim[3], Vincent Prevot[4], Barbara J Caldarone[5], Hyon Lee[1,6], and Young-Bum Kim[1#]

[1]Division of Endocrinology, Diabetes, and Metabolism, Department of Medicine, Beth Israel Deaconess Medical Center, and Harvard Medical School, Boston, MA, USA

[2]Department of Neurology, Brigham and Women's Hospital, Harvard Medical School, Boston, MA, USA

[3]The University of Sydney, Brain and Mind Centre, Sydney, NSW, Australia

[4]University Lille, Inserm, CHU Lille, Laboratory of Development and Plasticity of the Neuroendocrine Brain, Lille Neuroscience & Cognition, Lille, France

[5]Mouse Behavior Core, Department of Genetics, Harvard Medical School, Boston, MA, USA. Boston, Massachusetts, USA

[6]Department of Neurology, Gachon University Gil Medical Center, Incheon, Korea

[7]Department of Pathology, Faculty of Ceyhan Veterinary Medicine, Cukurova University, Adana, Turkey

*These authors contributed equally to this work

Running title: Role of LRP1 in GABAergic neurons

[#]Corresponding author: Young-Bum Kim, Ph.D.
Division of Endocrinology, Diabetes and Metabolism,
Beth Israel Deaconess Medical Center
330 Brookline Avenue, Boston, MA 02215
Phone: (617) 735-3252, Fax: (617) 735-3323
E-mail: ykim2@bidmc.harvard.edu

Abstract

Low-density lipoprotein receptor-related protein-1 (LRP1) plays an important role in regulating energy homeostasis, the integrity of the blood-brain barrier, and metabolic signal transport across the brain, while its dysfunction has been associated with cognitive decline, dementia, and Alzheimer's disease. However, the impact of LRP1 in GABAergic neurons on neurodegeneration and memory is poorly understood. Mice lacking LRP1 in GABAergic neurons (Vgat-Cre; LRP1$^{loxP/loxP}$) were subjected to behavioral tests for memory and learning. Here we show that the loss of LRP1 in GABAergic neurons causes significant impairment in short-term memory. The spatial Y-maze test revealed that Vgat-Cre; LRP1$^{loxP/loxP}$ mice exhibited decreased travel distance and duration in the novel arm compared to the controls (LRP1$^{loxP/loxP}$ mice). A reduction in correct responses to find the escape platform in the water T-maze test was found when LRP1 is absent in GABAergic neurons. Moreover, the distance and duration in the novel arm as well as the performance of the reversal water T-maze test were negatively correlated with body weight as well as serum levels of leptin, insulin, and ApoJ. Mice lacking LRP1 in GABAergic neurons displayed decreased freezing time in the contextual and cued fear conditioning test. Histopathological evaluation of the hippocampus revealed that Vgat-Cre; LRP1$^{loxP/loxP}$ mice had greater neuronal necrosis and neuroinflammation than those of LRP1$^{loxP/loxP}$ mice. These findings suggest that LRP1 in GABAergic neurons may play a crucial role in maintaining normal memory function and could be a molecular target for neurodegenerative diseases such as Alzheimer's disease.

Keywords: LRP1, GABAergic neurons, obesity, behavior, memory, neurodegeneration.

Introduction

Emerging data from human and animal studies suggest that obesity is linked to cognitive decline, brain atrophy, reduced white matter and integrity of the blood-brain barrier, and an elevated risk for late-onset AD [1-6]. Chronic disturbances in glucose homeostasis, impaired insulin signaling, and hypometabolism are highly correlated with cognitive impairment and AD pathogenesis [7-13]. We and others demonstrated that genetic disruption of low-density lipoprotein receptor-related protein 1 (LRP1) in the CNS or GABAergic neurons results in increased food intake, decreased energy expenditure, and metabolic changes leading to obesity [14, 15]. LRP1, a member of LDL receptor family, serves as a multi-ligand cell surface receptor and is broadly expressed in neurons [14, 16]. In addition to the important role of LRP1 in metabolism, LRP1 is also a major regulator of neurotransmission, synaptic plasticity, and clearance of the amyloid-β peptide [17-20]. LRP1 is also found to be crucial in the development of cognitive dysfunction and Alzheimer's disease (AD)-related dementia [21]. In particular, LRP1 levels were found to be markedly reduced in the brain of patients with AD, and decreased LRP1 levels correlate with increased AD susceptibility [22]. Deletion of LRP1 in endothelial cells of the brain led to a significant deficit in spatial learning and memory [23]. However, the impact of LRP1 dysfunction in GABAergic neurons on cognition is unknown.

In the current study, we investigated the role of LRP1 in GABAergic neurons in memory and cognitive function as well as the relationship between obesity-induced metabolic changes and behavioral outcomes. Here we show that GABAergic LRP1 plays a pivotal role in short-term memory function and neuronal degeneration in the context of obesity-linked metabolic dysfunction.

Results

Deletion of LRP1 from GABAergic neurons causes severe obesity

We previously reported that the deletion of LRP1 in GABAergic neurons leads to severe obesity by increasing food intake and decreasing energy expenditure and locomotor activity [14]. Consistently, we also observed that mice lacking LRP1 were severely obese (Fig. 1A) with an increased the amount of epididymal fat (Fig. 1B). Serum levels of leptin (Fig. 1C) and insulin (Fig. 1F) were also increased in Vgat-Cre; LRP1$^{loxP/loxP}$ mice compared with

LRP1$^{loxP/loxP}$ mice. However, neither serum FFA levels nor blood glucose levels were changed in Vgat-Cre; LRP1$^{loxP/loxP}$ mice (Fig. 1D–E). Vgat-Cre; LRP1$^{loxP/loxP}$ mice were insulin resistant, evidenced by an increased HOMA-IR index (Fig. G). These data demonstrate that LRP1 action in GABAergic neurons is required to regulate body-weight and metabolic homeostasis.

Mice lacking LRP1 in GABAergic neurons have increased serum ApoJ levels

Because elevated levels of serum ApoJ were found in humans with obesity and type 2 diabetes and diet-induced obese mice [24-26], we measured ApoJ levels in the serum and tissues of LRP1$^{loxP/loxP}$ mice and Vgat-Cre; LRP1$^{loxP/loxP}$ mice. Serum ApoJ levels in Vgat-Cre; LRP1$^{loxP/loxP}$ mice were significantly higher than those of LRP1$^{loxP/loxP}$ mice, but ApoJ levels in the liver, brain, hippocampus, and cerebral cortex were normal (Fig. 2A–E). Relationships between serum ApoJ levels and body weight, serum insulin, and leptin were observed (Fig. 2F–H). These findings indicate that increased serum ApoJ could contribute to the pathogenesis of LRP1-mediated metabolic disorders.

LRP1 in GABAergic neurons regulates motor function and spatial recognition memory

To determine whether GABAergic deletion of LRP1 alters motor activity and coordination, we performed open field and rotarod tests. Vgat-Cre; LRP1$^{\mathrm{loxP/loxP}}$ mice displayed a significant decrease in total travelled distance over 1 hour (Fig. 3A) and in 5 minutes interval (Fig. 3B) compared with LRP1$^{\mathrm{loxP/loxP}}$ mice. These effects were associate with reduced rotarod performance in Vgat-Cre; LRP1$^{\mathrm{loxP/loxP}}$ mice (Fig. 3C). We further performed the Y-maze test to see if LRP1 action in GABAergic neurons is involved in short term memory. Travel distance and time in the familiar arm were similar between LRP1$^{loxP/loxP}$ and Vgat-Cre; LRP1$^{loxP/loxP}$ mice (left panels of Fig. 3D and 3F), and the travel distance and time in the novel arm were increased compared with the familiar arm in both genotypes (right panels of Fig. 3D and 3F), indicating that the experiment works and mice in both groups have learning/memory skills. However, mice lacking LRP1 in GABAergic neurons visited novel arm less (Fig. 3D left panel and 3E) and spent less time there (Fig. 3F left panel and 3G) than LRP1$^{loxP/loxP}$ mice. These observations demonstrate that LRP1 in GABAergic neurons may play a role in regulating motor function and spatial short memory.

LRP1 in GABAergic neurons is involved in cognitive function

To further determine the impact of LRP1 action on cognitive function, we tested mice in the water T-maze and contextual and cued fear conditioning tasks (CCFC). During the water T-maze, the average percentage of correct responses to find the hidden escape platform decreased on the first day in Vgat-Cre; LRP1$^{loxP/loxP}$ mice, but no differences were seen on day 2 to 5 (Fig. 4A). Similar results were found when the escape platform was placed on the opposite side (Fig. 4B). Vgat-Cre; LRP1$^{loxP/loxP}$ mice that underwent CCFC showed a higher baseline freezing time on the training day than LRP1$^{loxP/loxP}$ mice. We therefore adjusted the results [including the training day, (Fig. 4C)] according to the baseline values of the training day. The adjusted data revealed that on the training day, all mice increased their freezing time slight or significantly on tone 2 and shock 2 compared to tone 1 and shock 1 (Fig. 4C), indicating a recognition of the neutral (tone) and aversive (shock) stimuli. However, Vgat-Cre; LRP1$^{loxP/loxP}$ mice exhibited less freezing time compared to the control mice on the second day during the contextual and cued fear conditioning tests (Fig. 4C). Together, these findings suggest that loss of LRP1 from GABAergic neurons leads to impairments in learning and short-term memory.

Perturbed metabolic profiles are associated with cognitive dysfunction in mice lacking LRP1 in GABAergic neurons

To determine the direct relationship between cognitive function and metabolic profiles, we performed correlation analyses between behavioral and metabolic parameters. Total travel distance and motor coordination negatively correlated with body weight (Fig. 5A–B). Total travel distance and duration in the novel arm tested by the Y-maze negatively correlated with important metabolic parameters, including body weight (Fig. 5C–D), serum insulin (Fig. 5E–F), leptin (Fig. 5G–H), and ApoJ (Fig. 5I). These results implicated a potential relationship between obesity and dysregulated locomotor activity, motor coordination, and spatial recognition memory.

Similar to the Y-maze correlation results, body weight (Fig. 6B), and the serum levels of leptin (Fig. 6D), insulin (Fig. 6F) and ApoJ (Fig. 6H) were found to be negatively correlated with the data from the reversal water T-maze. Serum ApoJ levels (Fig. 6G) also negatively correlated with the regular water T-maze, whereas body weight (Fig. 6A), serum leptin (Fig. 6C), and insulin (Fig. 6E) did not. These data indicate that perturbed metabolic outcomes

caused by LRP1 deletion in GABAergic neurons are associated with impaired cognitive function.

The impact of LRP1 on Aβ accumulation

Since GABAergic neuron-specific LRP1-deficient mice showed impairment in memory function, we measured Aβ levels in the serum, brain, and liver. The levels of $A\beta_{42}$ tended to be increased in the serum and brain of Vgat-Cre; LRP1$^{loxP/loxP}$ mice, but not in the liver compared with LRP1$^{loxP/loxP}$ mice (Fig. 7A–C). Serum and brain $A\beta_{40}$ levels tended to be decreased, while hepatic levels greatly increased in Vgat-Cre; LRP1$^{loxP/loxP}$ mice (Fig. 7D–F). The ratio of $A\beta_{42/40}$ was higher in Vgat-Cre; LRP1$^{loxP/loxP}$ mice than LRP1$^{loxP/loxP}$ mice (Fig. 7G). Deletion of LRP1 in GABAergic neurons tended to decrease hippocampal PSN1 levels while it had no effect on PSN1 levels in cortex and hippocampal APP levels (Fig. 7H–I).

Deficiency of LRP1 from GABAergic neurons leads to neuronal degeneration

We performed histopathological evaluation of the hippocampus to determine whether deleting LRP1 in GABAergic neurons induces neurodegeneration. Mice lacking LRP1 in GABAergic neurons showed necrotic changes such as neuronal shrinkage, darker cytoplasm and pycnosis in the hippocampus where mild microglial cell proliferation was also observed (Fig. 8A). In addition, Vgat-Cre; LRP1$^{loxP/loxP}$ mice had satellite microglial cells surrounding some neurons (called perineuronal satellitosis) in the hippocampus, whereas the control mice showed normal cell morphology without satellitosis (Fig. 8B). The quantifications of necrotic and glial cells and cells with satellitosis from the pathological images are shown in graphs.

We further performed immunohistochemistry (IHC) for GFAP, IBA1, GAD67, and NMDAR in the hippocampus of Vgat-Cre; LRP1$^{loxP/loxP}$ mice. The immunoreactivity of GFAP^{+}, IBA1^{+} and NMDAR^{+} neurons in hippocampus were significantly higher in Vgat-Cre; LRP1$^{loxP/loxP}$ mice than LRP1$^{loxP/loxP}$ mice (Fig. 8A–C). However, Vgat-Cre; LRP1$^{loxP/loxP}$ mice had decreased GAD67^{+} immunoreactivity compared to LRP1$^{loxP/loxP}$ mice (Fig. 8D). The quantitation data from the IHC images are shown in graphs. Collectively, these findings demonstrate that LRP1 deletion from GABAergic neurons induces neurodegeneration and causes significant immunohistochemical changes that may critically contribute to memory dysfunction and neurodegenerative pathogenesis.

Materials and Methods

Animal care

All animal care and experimental procedures were conducted in accordance with the National Institute of Health's Guide for the Care and the Use of Laboratory Animals and approved by the Institutional Animal Care and Use Committee of Beth Israel Deaconess Medical Center. Mice were allowed access to a standard chow diet (LabDiet, 5008 Formulab diet, Irradiated, cat no: 3003663-220) and water (reverse osmosis water) was provided *ad libitum*. They were housed at 22–24 °C with a 12-hour light-dark cycle with the light cycle starting from 6:00 a.m. to 6:00 p.m. Mice were single-housed in the same environmental conditions for behavioral studies.

Generation of Vgat-Cre; LRP1$^{loxP/loxP}$ mice

Mice bearing a *loxP*-flanked LRP1 allele (LRP1$^{loxP/loxP}$) were purchased from The Jackson Lab (Stock No: 012604, Bar Harbor, ME). Mice lacking LRP1 in Vgat-expressing neurons (Vgat-Cre; LRP1$^{loxP/loxP}$) were generated by mating LRP1$^{loxP/loxP}$ mice with Vgat-cre mice (gift from Dr. Brad Lowell, Beth Israel Deaconess Medical Center, Boston, MA). These mice were derived from 129 ES cells in C57BL/6 embryos. All mice studied were mixed background with 129 and C57BL/6. LRP1 expression was reduced in the arcuate nucleus, paraventricular hypothalamic nucleus, and dorsomedial hypothalamic nucleus of Vgat-Cre; LRP1$^{loxP/loxP}$ mice where Vgat is expressed [14].

Body weight and blood parameter measurements

Mice were weighed from 4 weeks of birth and weekly thereafter. Epidydimal fat was harvested and weighed at the end of experiment in male mice at 32 weeks of age. Blood was collected from overnight fasted mice via the tail. Blood glucose was measured using a OneTouch Ultra glucose meter (LifeScan, Inc., Milpitas, CA). Serum levels of insulin (90080, Crystal Chem, Chicago, IL), leptin (90030, Crystal Chem, Chicago, IL), ApoJ (MCLU00, R&D Systems, Minneapolis, MN), Aβ_{40} (KMB3481, Thermo Fisher Scientific Inc., Waltham, MA), Aβ_{42} (KMB3441, Thermo Fisher Scientific Inc., Waltham, MA) and free fatty acids (ab65341, Abcam, Waltham, MA) were measured by ELISA. HOMA-IR was calculated as [fasting glucose (mmol/L) × fasting insulin (μIU/mL)]/22.5 with a slight modification in insulin conversion as has recently been recommended [27, 28].

Immunoblotting analysis

Tissue lysates were resolved by sodium dodecyl sulfate–polyacrylamide gel electrophoresis (SDS–PAGE) and transferred to nitrocellulose membranes (GE Healthcare Life Sciences, Pittsburgh, PA). The membranes were incubated with polyclonal antibodies against presenilin-1 (sc-365450, Santa Cruz Biotechnology Inc., Dallas, TX) and amyloid precursor protein (APP) (A8717, Sigma-Aldrich, St. Louis, MO) or monoclonal antibody against β-actin (A2228, Sigma-Aldrich, Louis, MO). The membranes were washed with Tris-buffered saline (TBS) containing 0.1% Tween 20 for 30 min, incubated with horseradish peroxidase secondary antibodies against mouse (7076, Cell Signaling Technology, Danvers, MA) or rabbit (7074, Cell Signaling Technology) for 1 h, and washed with TBS containing 0.1% Tween 20 for 30 min. The bands were visualized with enhanced chemiluminescence and quantified by an ImageJ program (v1.52a, NIH). All protein levels were normalized by β-actin levels.

Open field test

Mice were placed in the center of a square Plexiglas box containing an invisible laser tracking system and allowed to freely explore the environment for 1 h. The total activity (cm) was recorded using specialized software (EthoVision XT 14, Noldus, Wageningen, the Netherlands).

Rotarod test

Mice were placed on a rotarod test apparatus (Ugo Basile, Gemonio, VA, Italy). Following an adaptation session of 5 min at 4 rpm, the acceleration of the rotating rod was set 4-40 rpm in 3 min. The time from beginning of the test until the mouse fell was recorded. The mice were tested again 3 h after the first test.

Morris water T-maze

A custom made Plexiglas plus maze testing apparatus (36 cm length, 10 cm width, 21 cm height) (Plastic Craft, West Nyack, NY) with four arms (North, South, East and West) was used to evaluate spatial memory. One arm was blocked off with a divider so that the mouse could choose one of the east and west arms to escape. An escape platform was placed on the east side of the maze ~ 1 cm below the surface water. The maze was filled with 23-26 ^{o}C water (renewed every trial) and white non-toxic paint to ensure that the mouse cannot see the escape platform. After a 10 min acclimation period in the testing room, the mice were placed

into the appropriate arm facing the wall, and they were allowed to swim until they found the escape platform. The start position was alternated (north and south) every trial. If the mouse was not able to find the escape platform within 2 min, the experimenter guided the mouse to the platform. The mice were allowed to stay on the platform for 10 sec before being placed back into their holding cages. After one day of training, mice were tested for 5 days (10 trials/day). Correct and incorrect choices to find the escape platform were recorded as 1 and 0, respectively. Once both knock-out and control mice reached the acquisition criteria, which was a group mean of 80% or more correct responses, the escape platform was moved to the opposite side (west) and reversal learning was conducted for 5 days.

Contextual and cued fear conditioning test

Mice were placed in Plexiglas conditioning chambers (Med associates, St. Albans, VT) with speakers (Med Associates Sound generator ENV-230, St. Albans, VT) and steel bars spaced 1 cm apart for electric shocks (0.5 mA). On the first day (training phase), after a 2-min acclimation period, the mice received two tones (30 sec) and electric shocks (2 sec) within the last two second of the tone with a 2-min inter-trial interval. On day 2, the mice were placed in the chamber, but did not receive a tone and electric shock. Freezing behavior was recorded and analyzed by the Ethovision Software (EthoVision XT 14, Noldus, Wageningen, the Netherlands) for the contextual fear conditioning experiment. After all mice were tested, the context was changed by inserting a white Plexiglas floor over the shock grid and white Plexiglas to cover the wall. Freezing was measured for 5 min in this altered context and for 3 min during presentation of the tone.

Histopathology

Mice were transcardially perfused with PBS followed by a 10% formalin solution. The brain samples obtained from the mice were further fixed in a 10% neutral formalin solution overnight and processed using graded alcohols and xylene. The samples were then embedded in paraffin, sectioned at 5 μm, stained with hematoxylin and eosin (H&E) (MHS32, Sigma-Aldrich, Louis, MO) and evaluated under a light microscope (Olympus BH-2, Shinjuku, Tokyo, Japan) for histopathological analysis [29]. Necrotic neurons with perineural satellitosis as well as microglial cells in the hippocampus were counted manually under a light microscope with the 40× magnification in 15 different areas for each section.

Immunohistochemical staining

IHC analysis was performed on 5-µm paraffin sections using the standard avidin–biotin–peroxidase complex (ABC) method according to the manufacturer's recommendations (Mouse and Rabbit Specific HRP/DAB (ABC) Detection IHC kit (ab64264) Abcam, Waltham, MA). Sections were subjected to routine deparaffinization in xylene and then rehydration in ethanol (100%, 80% and 50%). Inhibition of endogenous peroxidase activity and blocking of non-specific binding were performed according to the kit's instructions. Antigen retrieval for all markers was done by microwaving the sections in citrate buffer (pH = 6.0) at a sub-boiling temperature for 10 mins. After a second protein blocking, brain sections were incubated with primary antibodies overnight at 4 °C. The primary antibodies used were anti-glial fibrillary acidic protein (GFAP) antibody (dilution; 1:100, Sigma-Aldrich (G6171), St. Louis, MO), anti-ionized calcium binding adaptor molecule 1 (IBA1) antibody (dilution; 1:100, Wako (019-19741), Richmond, VA), anti-glutamic acid decarboxylase 67 (GAD67) antibody (clone 1G10.2, dilution; 1:100, Sigma-Aldrich (MAB5406)) and anti-N-methyl-D-aspartate receptor 1 (NMDAR1) antibody (dilution; 1:100, Abcam (ab193310)). The brown color of immunopositivity in brain sections was developed with 3,3'-diaminobenzidine tetrahydrochloride (DAB-H2O2) substrate in PBS for 5-min. Slides were counterstained with Mayer's hematoxylin (Sigma-Aldrich), dehydrated and mounted with Entellan (Sigma-Aldrich). On each slide, immunopositive reactions were detected by the presence of brown cytoplasmic staining. Immunopositive cells were counted as described in histopathology section.

Statistical analysis

The data were checked for the normality of distribution by the Shapiro-Wilk test. Logarithmic transformation or non-parametric tests were done if the data were not distributed normally. The student t-test or Mann-Whitney U test were conducted to compare two groups. The paired t-test or Wilcoxon test were used when comparing the data within groups. Two-way analysis of variance (ANOVA) was done when two independent factors [e.g. time-group or arm (familiar/novel)-group] might have an effect. Post hoc multiple comparisons were carried out using Sidak test in Graphpad Prism (GraphPad Prism, Version 8.0.1, La Jolla, CA) or general linear procedures in SPSS (extra coding were applied on the syntax menu) (SPSS 26.0 software for Windows; SPSS Inc., Chicago, IL). Correlations were done using Pearson's or Spearman correlation analyses depending on the data distribution. $P \leq 0.05$ was considered significant. The results were presented as mean ± standard error of mean (s.e.m.).

Discussion

We showed that LRP1 deficiency in GABAergic neurons, which is known to cause obesity and metabolic disturbances, alters locomotor activity and impairs short term memory. Changes in obesity-related metabolic parameters caused by LRP1 deletion in GABAergic neurons correlate with declining cognitive performance. Pathological and IHC analysis demonstrate that LRP1 in GABAergic neurons plays a pivotal role in the progression of neuronal degeneration. Thus, LRP1 in GABAergic neurons is an important regulator of memory and cognitive function.

Our study revealed that the specific deletion of LRP1 from GABAergic neurons led to moderate impairment of motor coordination and locomotor activity. This is consistent with previous studies using targeted deletion of LRP1 in the forebrain of mice, suggesting an important role for LRP1 in GABAergic neurons in motor function [30, 31]. However, previous studies demonstrated that reduction in motor coordination is also accompanied by increased adiposity, increased circulating insulin and leptin levels, and glucose intolerance [32, 33], and crosstalk between leptin and insulin signaling [34-36]. Moreover, while GABAergic LRP1 deleted mice were hypoactive and obese, non-obese mice with pan-neuronal LRP1 deletion exhibited hyperactive characteristics [31]. Thus, it is likely that neuronal dysfunction caused by GABAergic LRP1 deletion play a role in the development of motor abnormalities, along with impaired energy balance.

Obesity is associated with memory and learning deficits [37, 38]. One potential mechanism behind this suggests that excessive insulin causes an increased cerebral inflammatory response as well as increased Aβ levels, which may contribute to deleterious effects on working memory [39]. Supporting this, our memory behavior tests (water T-maze and fear conditioning) and correlation analysis collectively confirmed that hyperinsulinemia is correlated with poor memory performance. Likewise, transgenic AD mice developed glucose intolerance, hyperinsulinemia, memory impairment and increased insoluble amyloid-β protein deposition [40]. Moreover, immunohistochemical staining showed increased gliosis and neuronal death in obese GABAergic LRP1 deficient mice. Additionally, leptin has been shown to facilitate spatial learning and memory performance, and leptin deficiency led to impaired spatial memory in rodents [41-43]. In contrast, our LRP1-deficient mice with memory and learning deficits exhibited hyperleptinemia. Given that GABAergic LRP1-

deficient mice are obese but not leptin resistant [14], it is conceivable that leptin action in our animals may not be involved in learning and memory performance.

The fact that a lack of LRP1 in GABAergic neurons led to cognitive dysfunction may be associated with the neurodegeneration observed in the hippocampus. The majority (~80-90%) of the hippocampal neurons are principal cells, which are not GABAergic neurons. However, the inhibitory GABAergic neurons are highly heterogenic and show functionally diverse properties, allowing them to control spatio-temporal functions of the rest of the hippocampal cells [44, 45]. Thus, physiopathological and morphophysiological changes in these neurons may affect the overall hippocampal function. Accordingly, the present findings indicate that the lack of LRP1 in GABAergic neurons causes moderate-to-severe neurodegeneration as evidenced by the increased number of glial cells and cells with necrosis and satellitosis in the hippocampal area, confirmed by immunohistochemical analyses. Histopathological and immunohistochemical evaluations raised the question as to whether these cells are GABAergic neurons. Morphophysiologically, excitatory principal cells of the hippocampus are pyramidal neurons located in specific areas such as the stratum pyramidale while GABAergic interneurons are scattered throughout the hippocampus [46]. Thus, the neurodegeneration in the hippocampus was possibly involved both excitatory and GABAergic neurons which was expected due to regulatory function of GABAergic neurons on pyramidal neurons. Taken together, the cognitive dysfunction found in Vgat-Cre; LRP1$^{loxP/loxP}$ mice is likely due to the neurodegenerative changes in the hippocampus.

Another possible mechanism underlying the cognitive impairment seen in Vgat-Cre; LRP1$^{loxP/loxP}$ mice may involved the accumulation of Aβ in the brain. LRP1 in the brain plays a crucial role in regulating of Aβ production, as evidenced by the fact that the reduction in LRP1 expression is associated with Aβ clearence defect and accumulation [19-22]. The dynamic of $A\beta_{40}$ and $A\beta_{42}$ is the most important factor for modulating Aβ accumulation and clerance [47]. While $A\beta_{40}$ accounts for the most of the Aβ production, $A\beta_{42}$ is thought to trigger Aβ accumulation [47]. Therefore, changes in these two Aβ products provide critical information for Aβ accumulation. Even though inconsistencies have been reported [48], an increase in $A\beta_{42/40}$ ratio has been considered to contribute the Aβ accumulation in early onset Alzheimer's disease [49]. In this respect, our data show that mice lacking GABAergic LRP1 have increased serum and brain $A\beta_{42/40}$ ratio as described earlier in other AD models [48, 50,

51]. Thus, Aβ accumulation could be a factor for the progression of cognitive decline in mice lacking LRP1 in GABAergic neurons.

In conclusion, LRP1 deletion in GABAergic neurons resulted in behavior abnormalities, and memory and learning deficits. These effects were accompanied by neurodegeneration, neuroinflammation, and obesity. Thus, LRP1 in GABAergic neurons is an important regulator of memory and cognitive function.

Figure Legend

Figure 1. Selective deletion of LRP1 in GABAergic neurons causes metabolic disorders. (A) Body weight, (B) epididymal fat, (C) serum leptin, (D) serum FFA, (E) blood glucose, (F) serum insulin and (G) HOMA-IR of LRP1$^{loxP/loxP}$ and Vgat-Cre; LRP1$^{loxP/loxP}$ male mice. Body weight, epididymal fat, glucose, and serum parameters were measured from overnight fasted mice at 32 weeks of age. n = 12 for control, n = 18 for Vgat-Cre; LRP1$^{loxP/loxP}$. All graphs show means ± SEM. *p <0.05, ***p <0.001 vs. LRP1$^{loxP/loxP}$ by two-sided Student's t test or Mann-Whitney U test.

Figure 2. LRP1 deficiency in GABAergic neurons increases serum ApoJ levels. (A) Serum ApoJ (n = 12 for control, n = 18 for Vgat-Cre; LRP1$^{loxP/loxP}$), (B) liver ApoJ (n = 10 for control, n = 14 for Vgat-Cre; LRP1$^{loxP/loxP}$), (C) brain ApoJ (n = 5 for control, n = 7 for Vgat-Cre; LRP1$^{loxP/loxP}$), (D) hippocampus ApoJ (n = 5 for control, n = 5 for Vgat-Cre; LRP1$^{loxP/loxP}$), and (E) cerebral cortex ApoJ (n = 5 for control, n = 5 for Vgat-Cre; LRP1$^{loxP/loxP}$) of LRP1$^{loxP/loxP}$ and Vgat-Cre; LRP1$^{loxP/loxP}$ male mice. Relationship of serum ApoJ with (F) body weight, (G) serum insulin, and (H) serum leptin in LRP1$^{loxP/loxP}$ (n = 12) and Vgat-Cre; LRP1$^{loxP/loxP}$ (n = 18) male mice. ApoJ levels of serum and tissues were measured from overnight fasted mice at 32 weeks of age. The p values were obtained by Spearman correlation analysis and r values indicate Spearman correlation coefficient. All graph show means ± SEM. ***p <0.001 vs. LRP1$^{loxP/loxP}$ by two-sided Student's t test.

Figure 3. GABAergic neuron-specific deletion of LRP1 alters locomotor activity, motor coordination and spatial recognition memory. (A) Total distance travelled in 1 hour on the locomotion test, (B) distance travelled in 5 min intervals on the locomotion test, (C) latency to fall on the rotarod test, (D) total distance travelled in novel and familiar arms on the spatial Y-

maze test (left panel), and changes of total distance travelled from the familiar to novel arm (right panel), (E) percentage of distance travelled on the novel arm of spatial Y-maze. (F) time spent in the novel and familiar arms on the spatial Y-maze test (left panel), and changes in time spent from the familiar to novel arm (right panel), and (G) percentage of time spent in the novel arm of the spatial Y-maze. n = 12 for control, n = 18 for LRP1$^{loxP/loxP}$ (26 weeks old). All graphs show means ± SEM. *p <0.05, **p <0.01, ***p <0.001 vs. LRP1$^{loxP/loxP}$ by two-sided Student's t test. Data in right panels of D and F were evaluated by paired t-test.

Figure 4. Loss of LRP1 in GABAergic neurons leads to memory dysfunction. Percentage correct response (10 trials/day) of LRP1$^{loxP/loxP}$ (n = 10) and Vgat-Cre; LRP1$^{loxP/loxP}$ (n = 10) male mice (28-29 weeks old) on the (A) regular and (B) reversal water T-maze. *p <0.05, **p <0.01 by two-way analysis of variance (ANOVA) (*post hoc* tests were done using GLM procedures on SPSS). (C) Percentage fold change (relative to baseline) in freezing time of LRP1$^{loxP/loxP}$ (n = 10) and Vgat-Cre; LRP1$^{loxP/loxP}$ (n = 10) male mice (31 weeks old) during the fear conditioning test. All graphs show means ± SEM. *p <0.05 by two-sided Student's t test. #p <0.05 by paired t-test or Wilcoxon test. NS: Not significant.

Figure 5. Relationship of motor function, motor coordination and spatial recognition memory with obesity-linked metabolic parameters. Correlation of body weight with (A) total distance travelled on the locomotion test, (B) latency to fall on the rotarod test, (C) total distance travelled and (D) time spent in the novel arm on the spatial Y-maze test. Correlation of serum insulin with (E) total distance travelled and (F) time spent in the novel arm on the spatial Y-maze test. Correlation of serum leptin with (G) total distance travelled and (H) time spent in the novel arm on the spatial Y-maze test. (I) Correlation of serum ApoJ with time spent in the novel arm on the spatial Y maze test. The p values were obtained by Pearson correlation analysis and r values indicate Pearson correlation coefficient.

Figure 6. Relationship between metabolic parameters and cognitive function. Correlation of body weight, serum leptin, serum insulin, and serum ApoJ with the data from regular (A, C, E, G) and reversal (B, D, F, H) water T-maze on day 1. The p values were obtained by Pearson correlation analysis and r values indicate Pearson correlation coefficient.

Figure 7. $A\beta_{40}$, $A\beta_{42}$, APP and PSN1 levels in mice lacking LRP1 in GABAergic neurons. (A) Serum $A\beta_{42}$ level (n = 7 for control, n = 7 for Vgat-Cre; LRP1$^{loxP/loxP}$), (B) brain $A\beta_{42}$ level (n = 5 for control, n = 7 for Vgat-Cre; LRP1$^{loxP/loxP}$), (C) liver $A\beta_{42}$ level (n = 10 for control, n = 15 for Vgat-Cre; LRP1$^{loxP/loxP}$), (D) serum $A\beta_{40}$ level (n = 7 for control, n = 7 for Vgat-Cre; LRP1$^{loxP/loxP}$) (E) brain $A\beta_{40}$ level (n = 5 for control, n = 7 for Vgat-Cre; LRP1$^{loxP/loxP}$), (F) liver $A\beta_{42}$ level (n = 10 for control, n = 12 for Vgat-Cre; LRP1$^{loxP/loxP}$), and (G) serum $A\beta_{42/40}$ ratio of male LRP1$^{loxP/loxP}$ and Vgat-Cre; LRP1$^{loxP/loxP}$ male mice (32 weeks old). APP and PSN1 protein levels in (H) hippocampus and (I) cortex of LRP1$^{loxP/loxP}$ and Vgat-Cre; LRP1$^{loxP/loxP}$ mice. $A\beta_{42}$ and $A\beta_{40}$ levels in serum and tissues were measured from overnight fasted mice at 32 weeks of age. APP and PSN1 protein levels were assessed by immunoblotting. All graphs show means ± SEM. *p <0.05 vs. LRP1$^{loxP/loxP}$ by two-sided Student's t test or Mann-Whitney U test.

Figure 8. Histopathological features in the hippocampus of GABAergic neuron-specific LRP1-deficient mice. (A) Arrows indicate necrotic changes in neurons of Vgat-Cre; LRP1$^{loxP/loxP}$ mice. Normal neuronal appearance of LRP1$^{loxP/LoxP}$ mice was seen. (B) Arrow indicates a neuron with satellitosis in Vgat-Cre; LRP1$^{loxP/loxP}$ sample. No stelliotosis in LRP1$^{loxP/LoxP}$ mice were found. Necrotic neurons with perineural satellitosis as well as microglial cells in the hippocampus were counted manually from 5 serial sections. Graphs represent the quantitation of necrotic neuron number, glial cell number, and number of neurons with satellitosis in 15 areas/section. Scale bars represent 30 μm. All graphs show means ± SEM. *p <0.05, ***p <0.001 vs. LRP1$^{loxP/loxP}$ by two-sided Student's t test or Mann-Whitney U test. H&E: Hematoxylin and eosin.

Figure 9. Immunohistochemical analysis in the hippocampus of GABAergic neuron-specific LRP1-deficient mice. (A) GFAP, (B) IBA1, (C) NMDAR, and (D) GAD67 immunoreactivity of LRP1$^{loxP/loxP}$ (n = 7) and Vgat-Cre; LRP1$^{loxP/loxP}$ (n = 7) male mice. Arrows indicate GFAP^{+}, IBA1^{+}, NMDAR^{+}, and GAD67^{+} cells which were counted manually as described in Fig. 8. Graphs represent the quantitation of GFAP^{+}, IBA1^{+}, NMDAR^{+}, and GAD67^{+} cells in 15 areas/section. Scale bars represent 30 μm. All graphs show means ± SEM. **p <0.01, ***p <0.001 vs. LRP1$^{loxP/loxP}$ by two-sided Student's t test.

AUTHOR CONTRIBUTIONS

A.A.U., Z.S.H., and B.J.C. performed most of behavioral experiments. A.A. and J.K. performed histopathology and IHC experiments. K.R., J.Y., A.C., and W.M.Y. carried out blood serum parameters and immunoblotting analysis. A.A.U., W.K., V.P., Y.B.K. designed and planned the study. A.A.U., Z.S.H., H.L. and Y.B.K. wrote the manuscript with input from all other authors.

ACKNOWLEDGMENTS

This work was supported by grants from the National Institutes of Health (3R01DK106076-03S1 and 3R01 DK123002-02S1 to YBK). A.A. is a recipient of the fellowship from the Scientific and Technological Research Council of Turkey (TUBITAK, 1059B192100216) and K.C.R is a recipient of the fellowship from the São Paulo Research Foundation from Brazil (FAPESP 2019/19938-5). We thank Brad Lowell for Vgat-IRES-Cre recombinase mice, and all members of the Kim lab for their helpful advice and discussion. We are grateful to the Histology Core at Beth Israel Deaconess Medical Center.

CONFLICT OF INTEREST

The authors have no competing interests to declare.

REFERENCE

1. Anstey, K.J., et al., *Body mass index in midlife and late-life as a risk factor for dementia: a meta-analysis of prospective studies.* Obes Rev, 2011. **12**(5): p. e426-37.
2. Fitzpatrick, A.L., et al., *Midlife and late-life obesity and the risk of dementia: cardiovascular health study.* Arch Neurol, 2009. **66**(3): p. 336-42.
3. Jahn, H., *Memory loss in Alzheimer's disease.* Dialogues Clin Neurosci, 2013. **15**(4): p. 445-54.
4. Lane, C.A., J. Hardy, and J.M. Schott, *Alzheimer's disease*. Eur J Neurol, 2018. **25**(1): p. 59-70.
5. Profenno, L.A., A.P. Porsteinsson, and S.V. Faraone, *Meta-analysis of Alzheimer's disease risk with obesity, diabetes, and related disorders*. Biol Psychiatry, 2010. **67**(6): p. 505-12.
6. Serlin, Y., J. Levy, and H. Shalev, *Vascular pathology and blood-brain barrier disruption in cognitive and psychiatric complications of type 2 diabetes mellitus.* Cardiovasc Psychiatry Neurol, 2011. **2011**: p. 609202.
7. Cho, S., H. Lee, and J. Seo, *Impact of Genetic Risk Factors for Alzheimer's Disease on Brain Glucose Metabolism.* Mol Neurobiol, 2021. **58**(6): p. 2608-2619.
8. de Leon, M.J., et al., *Prediction of cognitive decline in normal elderly subjects with 2-[(18)F]fluoro-2-deoxy-D-glucose/poitron-emission tomography (FDG/PET).* Proc Natl Acad Sci U S A, 2001. **98**(19): p. 10966-71.

9. Drzezga, A., et al., *Cerebral metabolic changes accompanying conversion of mild cognitive impairment into Alzheimer's disease: a PET follow-up study.* Eur J Nucl Med Mol Imaging, 2003. **30**(8): p. 1104-13.
10. Gordon, B.A., et al., *Spatial patterns of neuroimaging biomarker change in individuals from families with autosomal dominant Alzheimer's disease: a longitudinal study.* Lancet Neurol, 2018. **17**(3): p. 241-250.
11. Liu, F., et al., *Reduced O-GlcNAcylation links lower brain glucose metabolism and tau pathology in Alzheimer's disease.* Brain, 2009. **132**(Pt 7): p. 1820-32.
12. Moloney, A.M., et al., *Defects in IGF-1 receptor, insulin receptor and IRS-1/2 in Alzheimer's disease indicate possible resistance to IGF-1 and insulin signalling.* Neurobiol Aging, 2010. **31**(2): p. 224-43.
13. Mosconi, L., et al., *Quantitation, regional vulnerability, and kinetic modeling of brain glucose metabolism in mild Alzheimer's disease.* Eur J Nucl Med Mol Imaging, 2007. **34**(9): p. 1467-79.
14. Kang, M.C., et al., *LRP1 regulates food intake and energy balance in GABAergic neurons independently of leptin action.* Am J Physiol Endocrinol Metab, 2021. **320**(2): p. E379-E389.
15. Liu, Q., et al., *Lipoprotein receptor LRP1 regulates leptin signaling and energy homeostasis in the adult central nervous system.* PLoS Biol, 2011. **9**(1): p. e1000575.
16. Fuentealba, R.A., et al., *Low density lipoprotein receptor-related protein 1 promotes anti-apoptotic signaling in neurons by activating Akt survival pathway.* J Biol Chem, 2009. **284**(49): p. 34045-53.
17. Bu, G., *Apolipoprotein E and its receptors in Alzheimer's disease: pathways, pathogenesis and therapy.* Nat Rev Neurosci, 2009. **10**(5): p. 333-44.
18. Lillis, A.P., et al., *LDL receptor-related protein 1: unique tissue-specific functions revealed by selective gene knockout studies.* Physiol Rev, 2008. **88**(3): p. 887-918.
19. Shibata, M., et al., *Clearance of Alzheimer's amyloid-ss(1-40) peptide from brain by LDL receptor-related protein-1 at the blood-brain barrier.* J Clin Invest, 2000. **106**(12): p. 1489-99.
20. Van Uden, E., et al., *Increased extracellular amyloid deposition and neurodegeneration in human amyloid precursor protein transgenic mice deficient in receptor-associated protein.* J Neurosci, 2002. **22**(21): p. 9298-304.
21. Fuentealba, R.A., et al., *Low-density lipoprotein receptor-related protein 1 (LRP1) mediates neuronal Abeta42 uptake and lysosomal trafficking.* PLoS One, 2010. **5**(7): p. e11884.
22. Kang, D.E., et al., *Modulation of amyloid beta-protein clearance and Alzheimer's disease susceptibility by the LDL receptor-related protein pathway.* J Clin Invest, 2000. **106**(9): p. 1159-66.
23. Storck, S.E., et al., *Endothelial LRP1 transports amyloid-beta(1-42) across the blood-brain barrier.* J Clin Invest, 2016. **126**(1): p. 123-36.
24. Kwon, M.J., et al., *Deficiency of clusterin exacerbates high-fat diet-induced insulin resistance in male mice.* Endocrinology, 2014. **155**(6): p. 2089-101.
25. Seo, J.A., et al., *Circulating ApoJ is closely associated with insulin resistance in human subjects*. Metabolism, 2018. **78**: p. 155-166.
26. Won, J.C., et al., *Plasma clusterin (ApoJ) levels are associated with adiposity and systemic inflammation.* PLoS One, 2014. **9**(7): p. e103351.
27. Knopp, J.L., L. Holder-Pearson, and J.G. Chase, *Insulin Units and Conversion Factors: A Story of Truth, Boots, and Faster Half-Truths.* J Diabetes Sci Technol, 2019. **13**(3): p. 597-600.

28. Matthews, D.R., et al., *Homeostasis model assessment: insulin resistance and beta-cell function from fasting plasma glucose and insulin concentrations in man.* Diabetologia, 1985. **28**(7): p. 412-9.
29. Luna, L.G., *anual of histologic staining methods of the Armed Forces Institute of Pathology*. 3rd Edition ed. 1968, New York: McGraw-Hill. 258.
30. Liu, Q., et al., *Neuronal LRP1 knockout in adult mice leads to impaired brain lipid metabolism and progressive, age-dependent synapse loss and neurodegeneration.* J Neurosci, 2010. **30**(50): p. 17068-78.
31. May, P., et al., *Neuronal LRP1 functionally associates with postsynaptic proteins and is required for normal motor function in mice.* Mol Cell Biol, 2004. **24**(20): p. 8872-83.
32. Stojakovic A, M.C., Licinio J, Wong M-Li *Long-term consumption of high-fat diet impairs motor coordination without affecting the general motor activity*. J Transl Sci, 2019. **5**(5).
33. Smith, S.M., et al., *Aging-Related Behavioral, Adiposity, and Glucose Impairments and Their Association following Prenatal Alcohol Exposure in the C57BL/6J Mouse.* Nutrients, 2022. **14**(7).
34. Huo, L., et al., *Leptin-dependent control of glucose balance and locomotor activity by POMC neurons.* Cell Metab, 2009. **9**(6): p. 537-47.
35. Sartorius, T., et al., *Leptin affects insulin action in astrocytes and impairs insulin-mediated physical activity.* Cell Physiol Biochem, 2012. **30**(1): p. 238-46.
36. Wang, C., et al., *Obesity Reduces Cognitive and Motor Functions across the Lifespan.* Neural Plast, 2016. **2016**: p. 2473081.
37. Coppin, G., et al., *Working memory and reward association learning impairments in obesity.* Neuropsychologia, 2014. **65**: p. 146-55.
38. Gunstad, J., et al., *Obesity is associated with memory deficits in young and middle-aged adults.* Eat Weight Disord, 2006. **11**(1): p. e15-9.
39. Craft, S., *Insulin resistance syndrome and Alzheimer's disease: age- and obesity-related effects on memory, amyloid, and inflammation.* Neurobiol Aging, 2005. **26 Suppl 1**: p. 65-9.
40. Cao, D., et al., *Intake of sucrose-sweetened water induces insulin resistance and exacerbates memory deficits and amyloidosis in a transgenic mouse model of Alzheimer disease.* J Biol Chem, 2007. **282**(50): p. 36275-82.
41. Li, X.L., et al., *Impairment of long-term potentiation and spatial memory in leptin receptor-deficient rodents*. Neuroscience, 2002. **113**(3): p. 607-15.
42. Oomura, Y., S. Aou, and K. Fukunaga, *Prandial increase of leptin in the brain activates spatial learning and memory.* Pathophysiology, 2010. **17**(2): p. 119-27.
43. Oomura, Y., et al., *Leptin facilitates learning and memory performance and enhances hippocampal CA1 long-term potentiation and CaMK II phosphorylation in rats.* Peptides, 2006. **27**(11): p. 2738-49.
44. Booker, S.A. and I. Vida, *Morphological diversity and connectivity of hippocampal interneurons.* Cell Tissue Res, 2018. **373**(3): p. 619-641.
45. Cobb, S., et al., *Hippocampal Microcircuits : A Computational Modeler's Resource Book*, in *Springer Series in Computational Neuroscience*,. p. 1 online resource (XVII, 879 pages 182 illustrations, 120 illustrations in color.).
46. Pelkey, K.A., et al., *Hippocampal GABAergic Inhibitory Interneurons.* Physiol Rev, 2017. **97**(4): p. 1619-1747.
47. Kelleher, R.J., 3rd and J. Shen, *Presenilin-1 mutations and Alzheimer's disease.* Proc Natl Acad Sci U S A, 2017. **114**(4): p. 629-631.

48. Sun, L., et al., *Analysis of 138 pathogenic mutations in presenilin-1 on the in vitro production of Abeta42 and Abeta40 peptides by gamma-secretase.* Proc Natl Acad Sci U S A, 2017. **114**(4): p. E476-E485.
49. Selkoe, D.J. and J. Hardy, *The amyloid hypothesis of Alzheimer's disease at 25 years*. EMBO Mol Med, 2016. **8**(6): p. 595-608.
50. Wolfe, M.S., *When loss is gain: reduced presenilin proteolytic function leads to increased Abeta42/Abeta40. Talking Point on the role of presenilin mutations in Alzheimer disease.* EMBO Rep, 2007. **8**(2): p. 136-40.
51. Xia, D., et al., *Presenilin-1 knockin mice reveal loss-of-function mechanism for familial Alzheimer's disease*. Neuron, 2015. **85**(5): p. 967-81.

Fig. 1

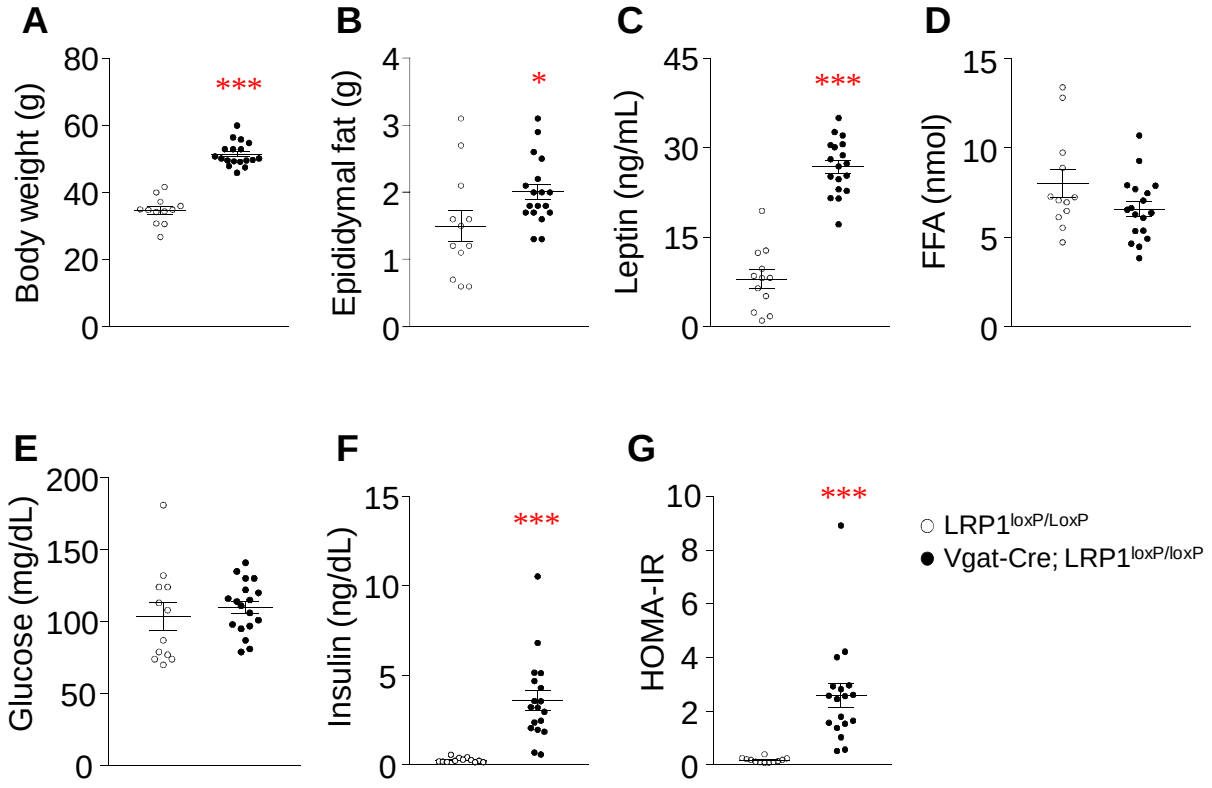
A
Body weight (g)
80
60
40
20
0
***
B
Epididymal fat (g)
4
3
2
1
0
*
C
Leptin (ng/mL)
45
30
15
0
***
D
FFA (nmol)
15
10
5
0
E
Glucose (mg/dL)
200
150
100
50
0
F
Insulin (ng/dL)
15
10
5
0
***
G
HOMA-IR
10
8
6
4
2
0
***
LRP1loxP/LoxP
Vgat-Cre; LRP1loxP/loxP

Fig. 2

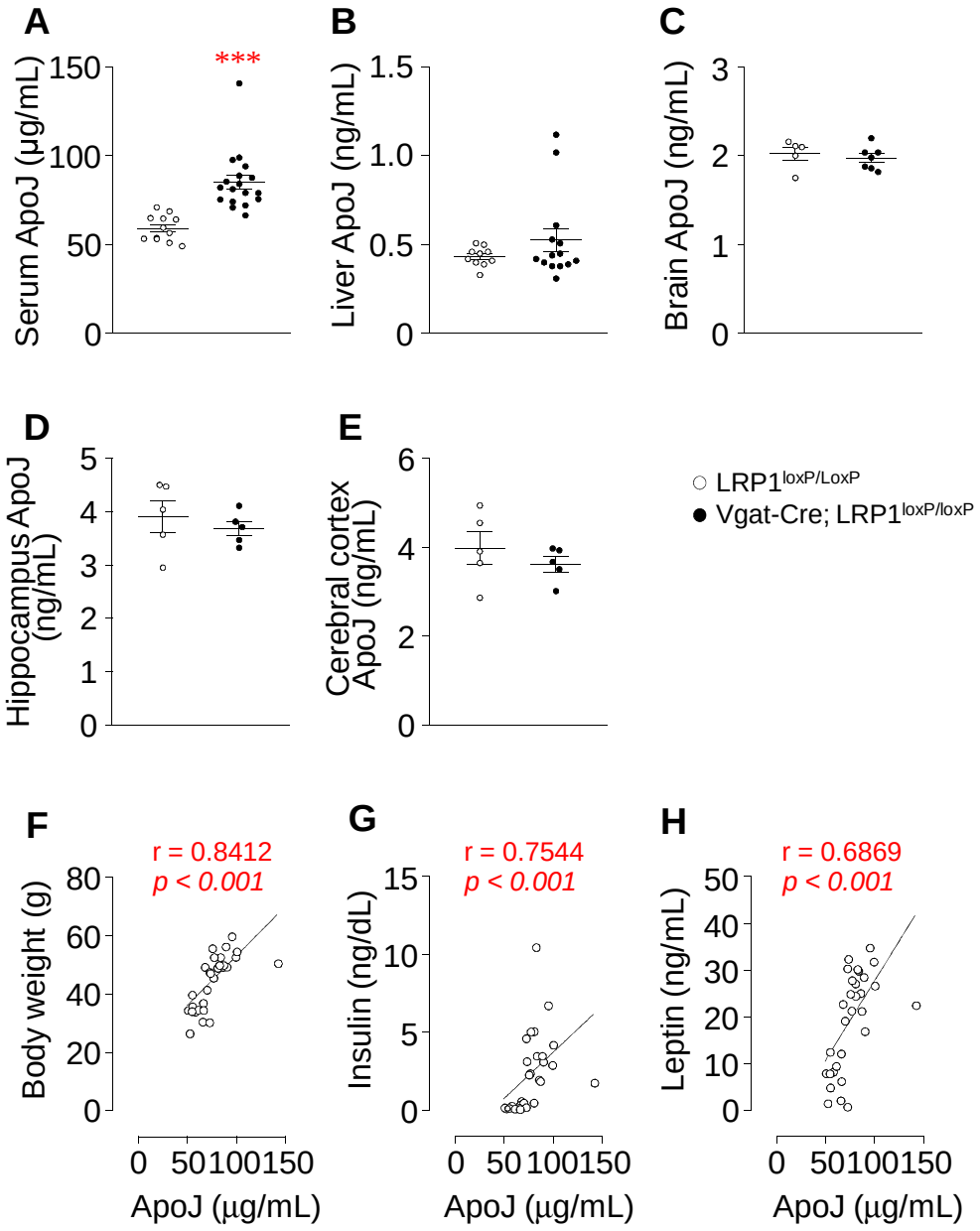
A
B
C
D
E
F
G
H
Serum ApoJ (μg/mL)
Liver ApoJ (ng/mL)
Brain ApoJ (ng/mL)
Hippocampus ApoJ (ng/mL)
Cerebral cortex ApoJ (ng/mL)
Body weight (g)
Insulin (ng/dL)
Leptin (ng/mL)
***
r = 0.8412
p < 0.001
r = 0.7544
p < 0.001
r = 0.6869
p < 0.001
ApoJ (μg/mL)
LRP1loxP/LoxP
Vgat-Cre; LRP1loxP/loxP

Fig. 3

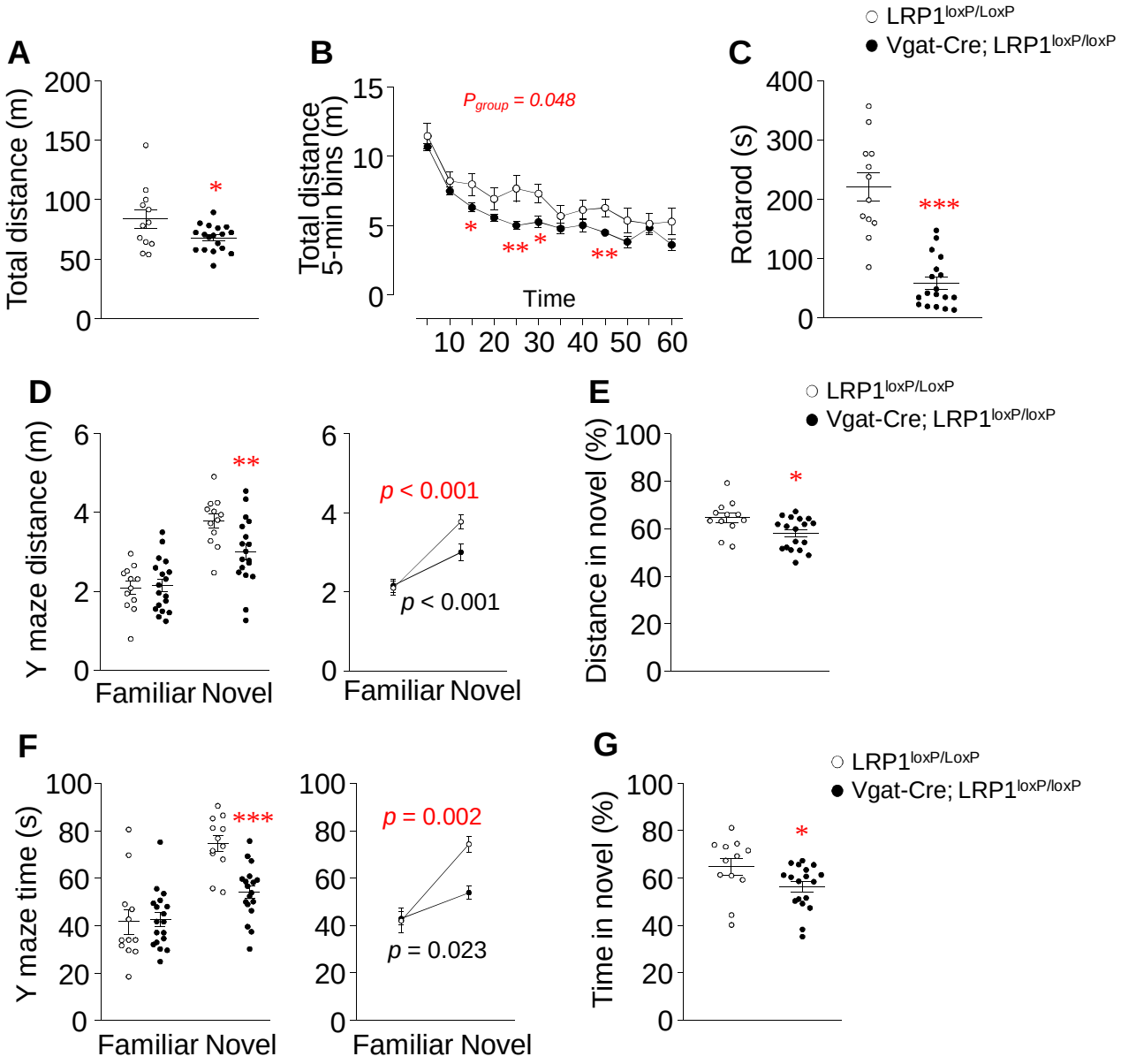
A
Total distance (m)
200
150
100
50
0
*
B
Total distance 5-min bins (m)
15
10
5
0
P_{group} = 0.048
*
**
*
**
Time
10 20 30 40 50 60
C
Rotarod (s)
400
300
200
100
0
***
LRP1loxP/LoxP
Vgat-Cre; LRP1loxP/loxP
D
Y maze distance (m)
6
4
2
0
**
Familiar Novel
p < 0.001
p < 0.001
Familiar Novel
E
Distance in novel (%)
100
80
60
40
20
0
*
LRP1loxP/LoxP
Vgat-Cre; LRP1loxP/loxP
F
Y maze time (s)
100
80
60
40
20
0
***
Familiar Novel
p = 0.002
p = 0.023
Familiar Novel
G
Time in novel (%)
100
80
60
40
20
0
*
LRP1loxP/LoxP
Vgat-Cre; LRP1loxP/loxP

Fig. 4

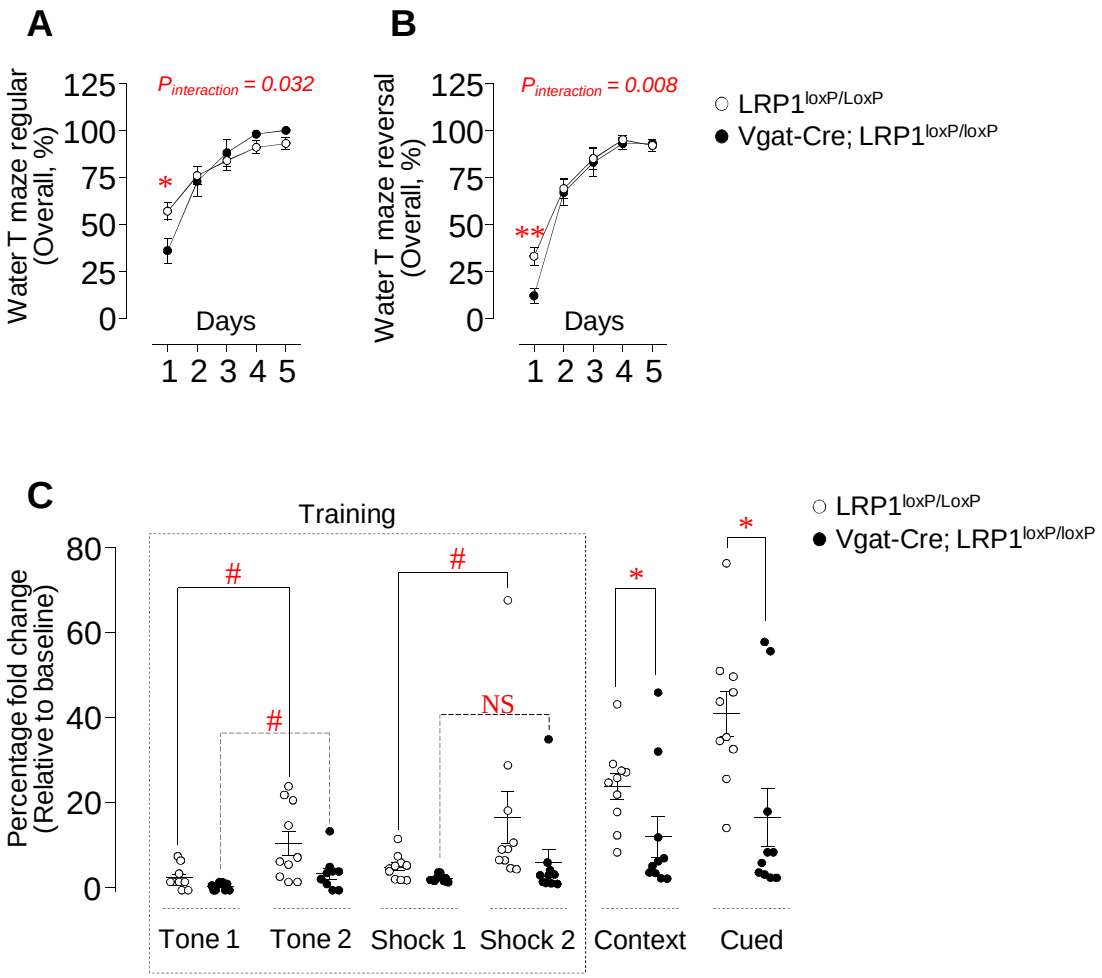
A
B
C
Water T maze regular (Overall, %)
Water T maze reversal (Overall, %)
Percentage fold change (Relative to baseline)
$P_{interaction}$ = 0.032
$P_{interaction}$ = 0.008
Days
Training
Tone 1
Tone 2
Shock 1
Shock 2
Context
Cued
NS
LRP1loxP/LoxP
Vgat-Cre; LRP1loxP/loxP

Fig. 5

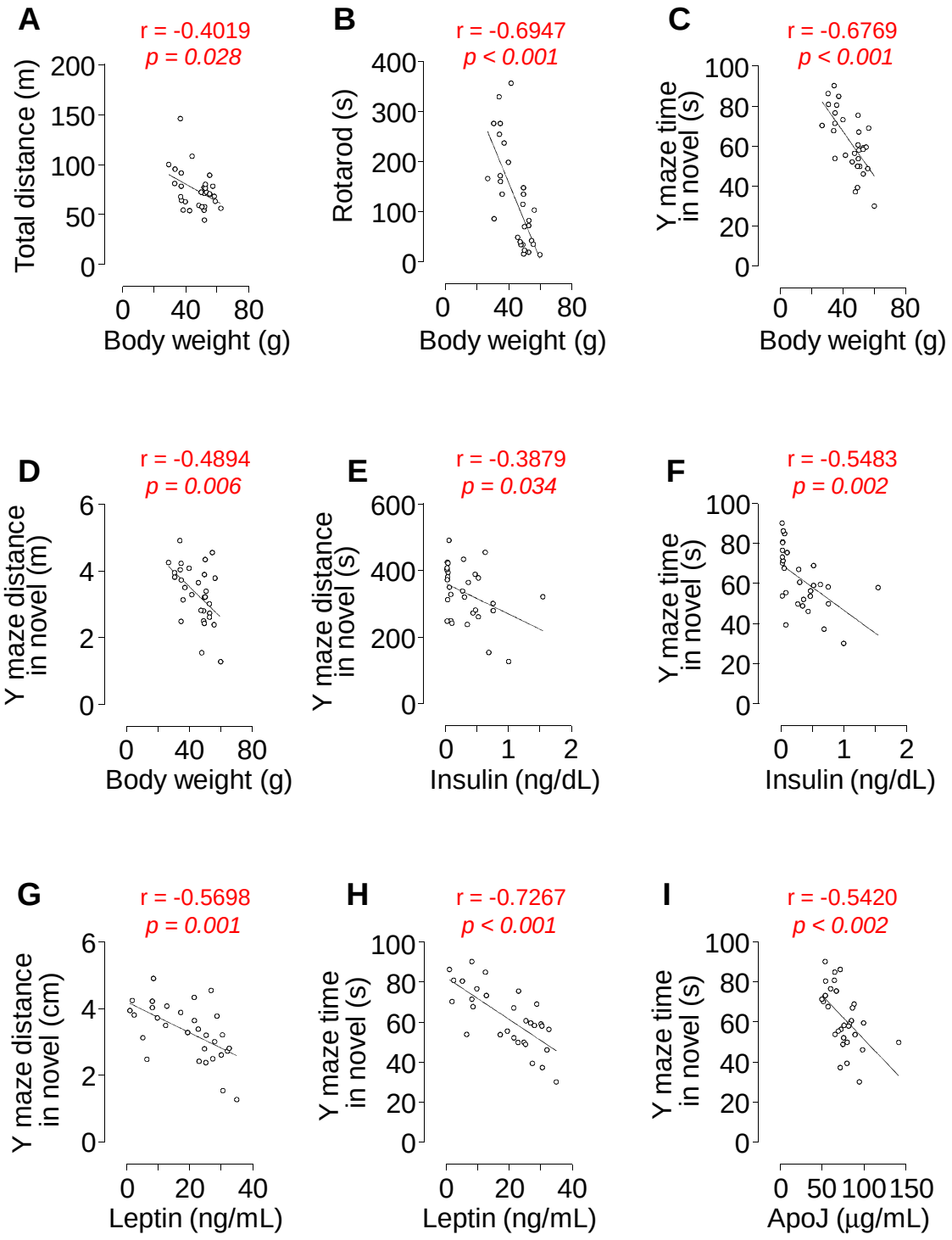
A
r = -0.4019
p = 0.028
Total distance (m)
Body weight (g)
B
r = -0.6947
p < 0.001
Rotarod (s)
Body weight (g)
C
r = -0.6769
p < 0.001
Y maze time in novel (s)
Body weight (g)
D
r = -0.4894
p = 0.006
Y maze distance in novel (m)
Body weight (g)
E
r = -0.3879
p = 0.034
Y maze distance in novel (s)
Insulin (ng/dL)
F
r = -0.5483
p = 0.002
Y maze time in novel (s)
Insulin (ng/dL)
G
r = -0.5698
p = 0.001
Y maze distance in novel (cm)
Leptin (ng/mL)
H
r = -0.7267
p < 0.001
Y maze time in novel (s)
Leptin (ng/mL)
I
r = -0.5420
p < 0.002
Y maze time in novel (s)
ApoJ (μg/mL)

Fig. 6

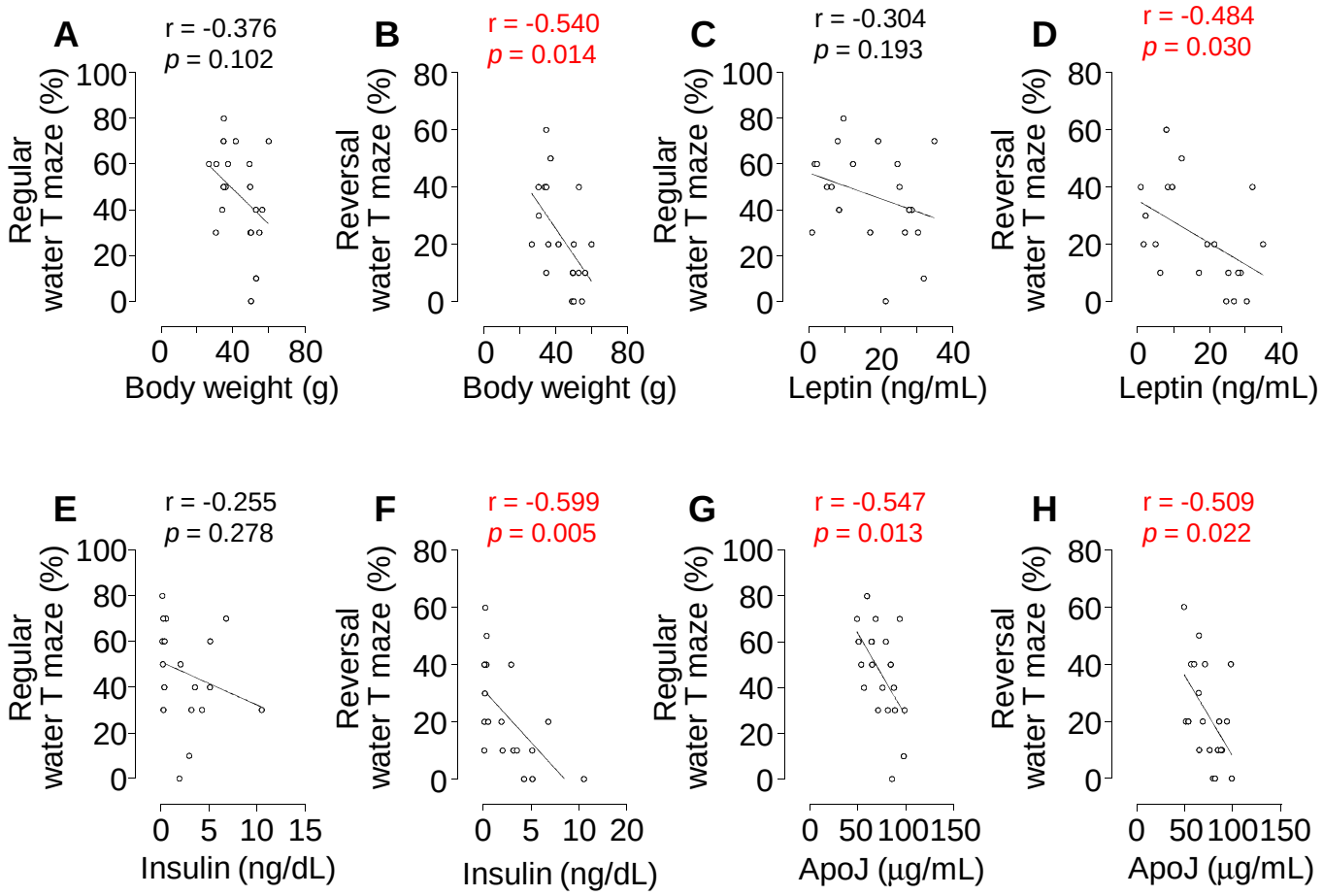
A
r = -0.376
p = 0.102
Regular water T maze (%)
Body weight (g)
B
r = -0.540
p = 0.014
Reversal water T maze (%)
Body weight (g)
C
r = -0.304
p = 0.193
Regular water T maze (%)
Leptin (ng/mL)
D
r = -0.484
p = 0.030
Reversal water T maze (%)
Leptin (ng/mL)
E
r = -0.255
p = 0.278
Regular water T maze (%)
Insulin (ng/dL)
F
r = -0.599
p = 0.005
Reversal water T maze (%)
Insulin (ng/dL)
G
r = -0.547
p = 0.013
Regular water T maze (%)
ApoJ (µg/mL)
H
r = -0.509
p = 0.022
Reversal water T maze (%)
ApoJ (µg/mL)

Fig. 7

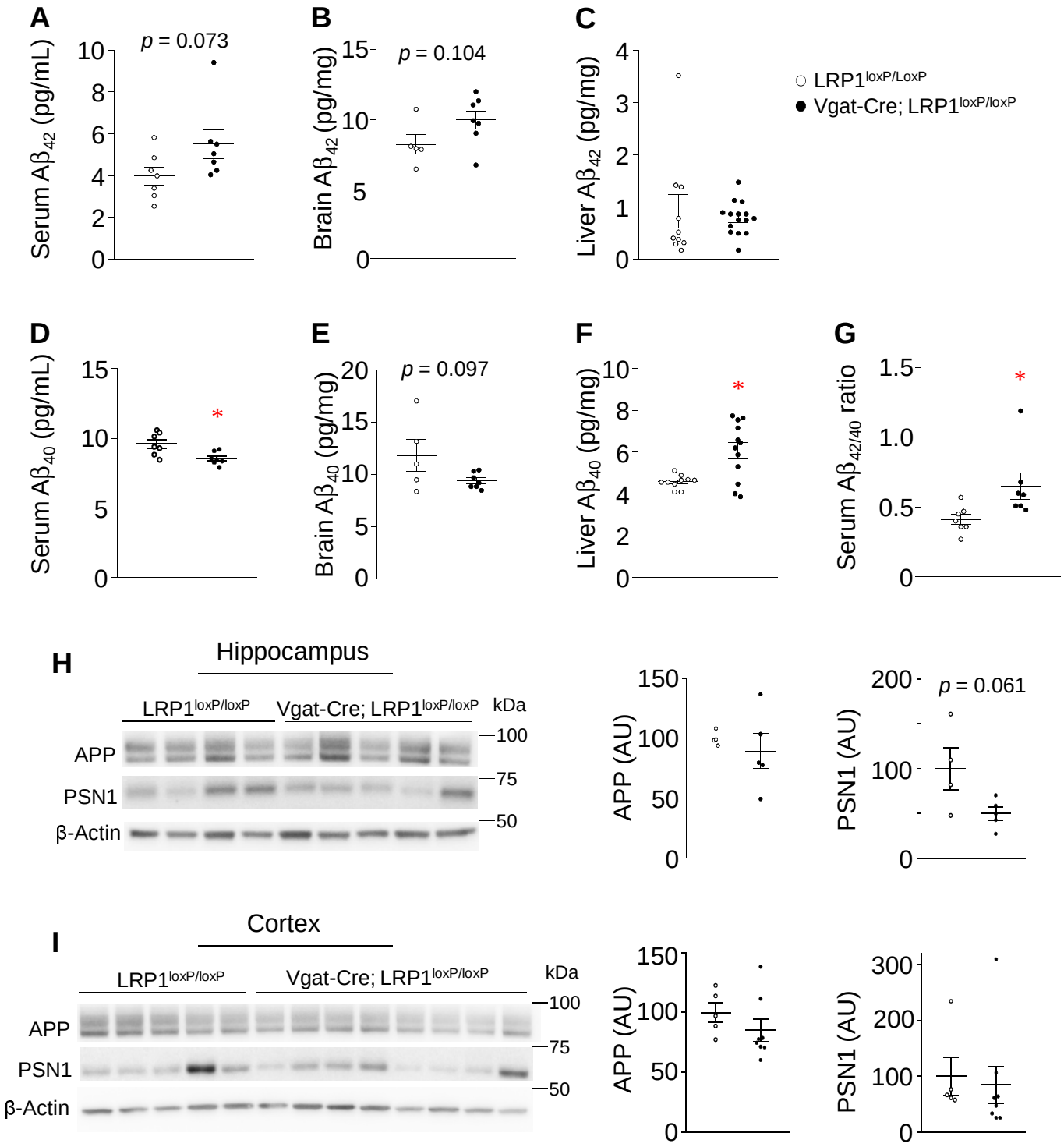
A
Serum Aβ42 (pg/mL)
p = 0.073
B
Brain Aβ42 (pg/mg)
p = 0.104
C
Liver Aβ42 (pg/mg)
LRP1loxP/LoxP
Vgat-Cre; LRP1loxP/loxP
D
Serum Aβ40 (pg/mL)
E
Brain Aβ40 (pg/mg)
p = 0.097
F
Liver Aβ40 (pg/mg)
G
Serum Aβ42/40 ratio
H
Hippocampus
LRP1loxP/loxP
Vgat-Cre; LRP1loxP/loxP
kDa
APP
PSN1
β-Actin
APP (AU)
PSN1 (AU)
p = 0.061
I
Cortex

Fig. 8

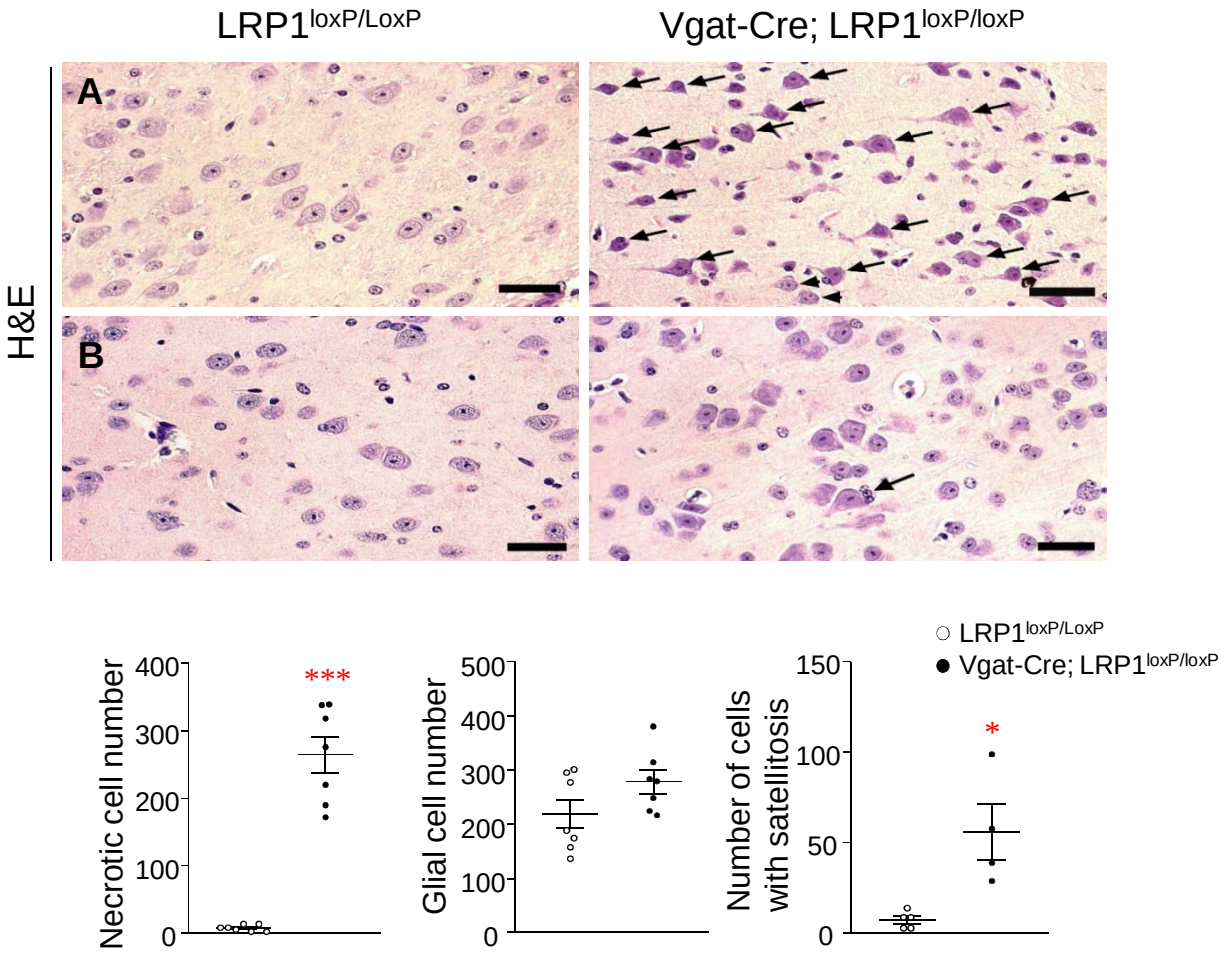
LRP1loxP/LoxP
Vgat-Cre; LRP1loxP/loxP
H&E
A
B
Necrotic cell number
400
300
200
100
0
***
Glial cell number
500
400
300
200
100
0
Number of cells with satellitosis
150
100
50
0
*
LRP1loxP/LoxP
Vgat-Cre; LRP1loxP/loxP

Fig. 9

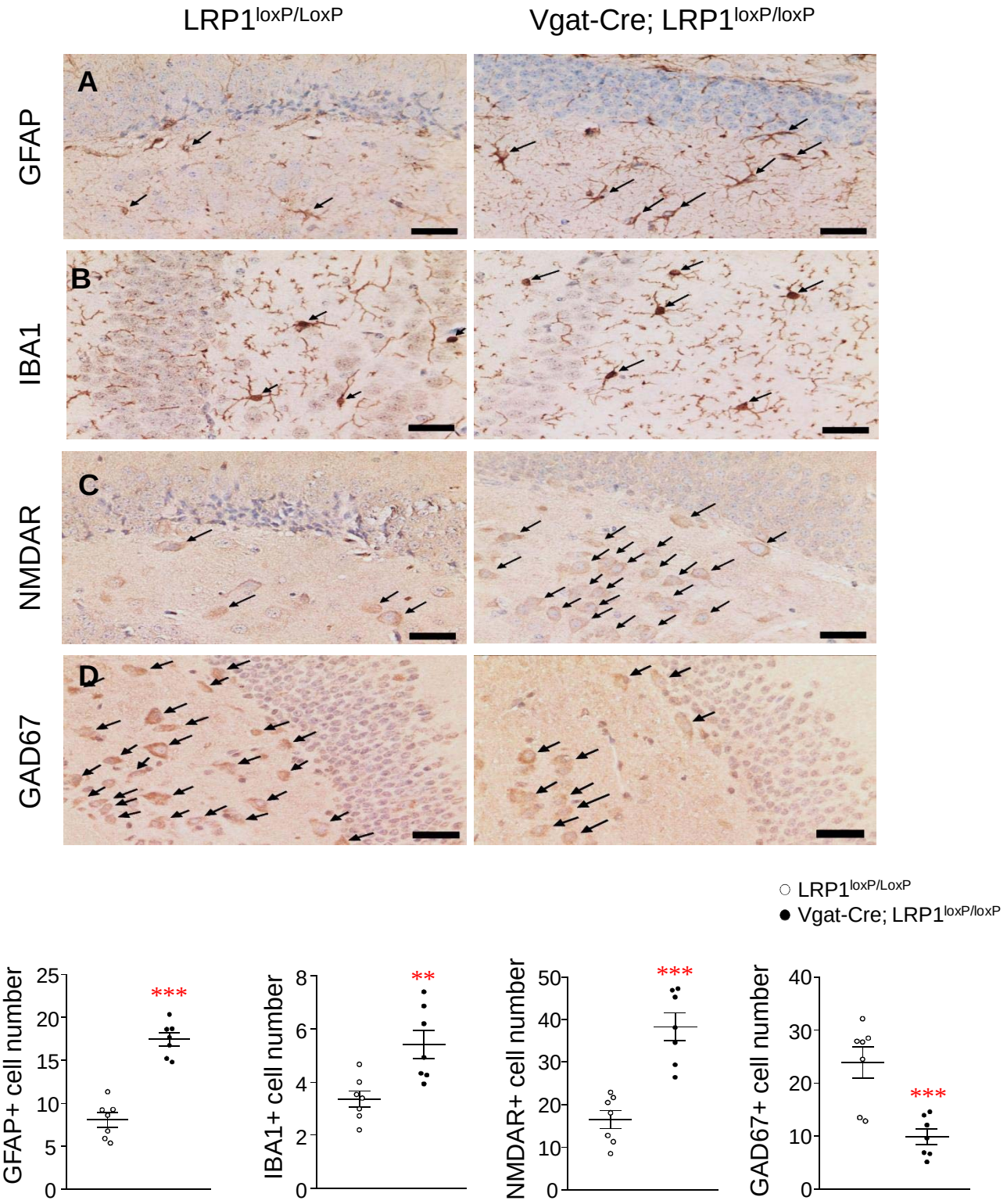
LRP1loxP/LoxP
Vgat-Cre; LRP1loxP/loxP
A
B
C
D
GFAP
IBA1
NMDAR
GAD67
LRP1loxP/LoxP
Vgat-Cre; LRP1loxP/loxP
GFAP+ cell number
IBA1+ cell number
NMDAR+ cell number
GAD67+ cell number
***
**
***
***